Atmos. Chem. Phys. Discuss., doi:10.5194/acp-2016-964, 2016
Manuscript under review for journal Atmos. Chem. Phys.
Published: 8 November 2016

Atmospheric Chemistry and Physics Discussions

Testing chemistry-climate models' regulation of tropical lower-stratospheric water vapor

Kevin M. Smalley[1], Andrew E. Dessler[1], Slimane Bekki[2], Makoto Deushi[3], Marion Marchand[2], Olaf Morgenstern[4], David A. Plummer[5], Kiyotaka Shibata[6], Yousuke Yamashita[7,8], and Guang Zeng[4]

[1]Department of Atmospheric Science, Texas A&M, College Station, Texas, USA.
[2]LATMOS, Institut Pierre Simon Laplace (IPSL), Paris, France
[3]Meteorological Research Institute, 1-1 Nagamine, Tsukuba, Ibaraki 305-0052, Japan
[4]National Institute of Water and Atmospheric Research (NIWA), Lauder, New Zealand
[5]Canadian Centre for Climate Modelling and Analysis, Environment and Climate Change Canada
[6]School of Environmental Science and Engineering, Kochi University of Technology
[7]National institute for Environmental Studies (NIES)
[8]Now at Japan Agency for Marine-Earth Science and Technology (JAMSTEC), Yokohama, Japan

Correspondence to: Andrew Dessler (adessler@tamu.edu)

Abstract. Climate models predict that tropical lower stratospheric humidity will increase as the climate warms, with important implications for the chemistry and climate of the atmosphere. We analyze the trend in 21^{st}-century simulations from 12 state-of-the-art chemistry-climate models (CCMs) using a linear regression model to determine the factors driving the trends. Within CCMs, the long-term trend in humidity is primarily driven by warming of the troposphere. This is partially offset in most CCMs by an increase in the strength of the Brewer-Dobson circulation, which tends to cool the tropical tropopause layer (TTL). We also apply the regression model to individual decades from the 21^{st} century CCM runs and compare them to observations. Many of the CCMs, but not all, compare well with observations, lending credibility to their predictions. One notable deficiency in most CCMs is that they underestimate the impact of the quasi-biennial oscillation on lower stratospheric humidity. Our analysis provides a new and potentially superior way to evaluate model trends in lower stratospheric humidity.

1 Introduction

Variations of stratospheric water vapor can impact both the climate and chemistry of the atmosphere. Because of this, understanding the processes that control the humidity of air entering the tropical lower stratosphere (hereafter $[H_2O]_{entry}$) has been a high priority of the scientific community since Brewer (1949) first described the stratospheric circulation.

It is now well established that the fundamental control over $[H_2O]_{entry}$ comes from the cold temperatures found in the tropical tropopause layer (TTL) (Fueglistaler et al., 2009b) and that variability in these temperatures translates into variability in $[H_2O]_{entry}$. The most well-known example of this is the so-called "tape recorder," in which the seasonal cycle in TTL temperatures is imprinted on tropical stratospheric water vapor (Mote et al., 1996).

On interannual time scales, variability in $[H_2O]_{entry}$ originates from processes such as the Brewer-Dobson Circlation (BDC) and the quasi-biennial oscillation (QBO). More recently, Dessler et al. (2013, 2014) has suggested that the temperature of the

Atmos. Chem. Phys. Discuss., doi:10.5194/acp-2016-964, 2016
Manuscript under review for journal Atmos. Chem. Phys.
Published: 8 November 2016

Atmospheric Chemistry and Physics Discussions

troposphere also exerts an influence on $[H_2O]_{entry}$. This implies the existence of a stratospheric water vapor feedback, whereby a warming climate would increase stratospheric water vapor, leading to further warming.

Putting these factors together, Dessler et al. (2013, 2014) demonstrated that observed $[H_2O]_{entry}$ could be accurately reproduced with a simple linear model:

$$[H_2O]_{entry} = \beta_0 + \beta_{\Delta T}\Delta T + \beta_{BDC}BDC + \beta_{QBO}QBO + \epsilon \quad (1)$$

Where ΔT is the temperature of the troposphere, BDC is the strength of the Brewer-Dobson circulation, QBO represents the phase of the QBO, and epsilon is the residual. As expected, they found that a stronger BDC, which tends to cool the TTL, reduces $[H_2O]_{entry}$; this is consistent with previous analyses (Brewer, 1949; Randel et al., 2006; Castanheira et al., 2012; Fueglistaler et al., 2014; Gilford et al., 2016). They also found that the QBO introduces significant variability with a time scale of a few years, also consistent with previous work (O'Sullivan and Dunkerton, 1997; Randel et al., 1998; Dunkerton, 2001; Fueglistaler and Haynes, 2005; Choiu et al., 2006; Liang et al., 2011; Castanheira et al., 2012; Khosrawi et al., 2013; Kawatani et al., 2014; Tao et al., 2015). Finally, a warmer troposphere tends to increase $[H_2O]_{entry}$, although whether this is through influence on TTL temperatures or some other mechanism, such as convective ice lofting, is not clear.

Virtually all climate models predict that $[H_2O]_{entry}$ will increase as the climate warms. Dessler et al. (2013) analyzed one chemistry-climate model (CCM) to better understand this trend (CCMs are similar to general circulation models, but with a more realistic stratosphere and higher vertical resolution in the TTL) and found that the regression model worked well in reproducing the CCM's $[H_2O]_{entry}$ trend over the 21^{st} century. They further found that the increase in $[H_2O]_{entry}$ was driven by the increase in tropospheric temperatures, which was partially offset by a strengthening BDC.

Dessler et al. (2013)'s analysis provided a novel way to examine the regulation of $[H_2O]_{entry}$ in CCMs and compare it to observations. The purpose of this paper is to use this technique to examine a set of CCMs, with the goal of providing insight into the realism of the models.

2 Models

We analyze model output from 7 CCMs participating in Phase 2 of the Chemistry-Climate Model Validation Project (CCMVal-2) (Morgenstern et al. (2010); SPARC (2010)) and output from 5 CCMs participating in Phase 1 of the Chemistry-Climate Model Initiative (CCMI-1) (Morgenstern et al. (2016)). Table 1 lists the models.

We use simulations from the REF-B2 scenario of CCMVal-2. In this scenario, greenhouse gas concentrations during the 21^{st} century come from the A1B scenario, which lies in the middle of the SRES scenarios (IPCC, 2001). Ozone-depleting substance come from the halogen emission scenario A1 described by (WMO, 2007). CCMVal-2 specifics can be found inSPARC (2010) and Morgenstern et al. (2010). We use the refC2 scenario of the CCMI-1. In this scenario, greenhouse gas concentrations come from the RCP 6.0 scenario (Meinshausen et al., 2011) and ozone-depleting substances come from the halogen emission scenario A1 described described by (WMO, 2014). CCMI-1 model specifics can be found in Morgenstern et al. (2016). In

Atmos. Chem. Phys. Discuss., doi:10.5194/acp-2016-964, 2016
Manuscript under review for journal Atmos. Chem. Phys.
Published: 8 November 2016

Atmospheric Chemistry and Physics Discussions

order to maintain a consistent reference period between models, our analysis covers 2000-2097, which we will hereafter refer to as "the 21^{st} century ".

For each model, we fit CCM $[H_2O]_{entry}$ using the multivariate linear regression (MLR) model described above. We use tropical average 80-hPa water vapor volume mixing ratio anomaly as a proxy for $[H_2O]_{entry}$ (all tropical averages in this paper are averages over 30°N-30°S; anomalies are calculated by subtracting off the mean annual cycle from the time series). For our BDC index, we use 80-hPa diabatic heating rate anomalies (see Fueglistaler et al. (2009a) for details). The tropospheric temperature index is the 500-hPa tropical average temperature anomaly, and for the few CCMI-1 simulations that only produce variables on hybrid pressure levels (CMAM, CCSRNIES-MIROC3.2, and MRI-ESM1r1), we choose a hybrid pressure level close to the 500-hPa pressure surface (See Table 1). All of these choices are similar to those used by Dessler et al. (2013, 2014).

For the QBO index, we take the standardized anomaly of equatorial 50-hPa zonal winds. By examining 21^{st} century 50 hPa zonal winds (shown in supplement figures), we find that only 5 of the 12 models simulate a QBO (table 1). As a result, we do not expect the QBO to significantly impact $[H_2O]_{entry}$ in all of the models.

The MLR returns the coefficients for each regression coefficient in Equation 1, along with an uncertainty for each coefficient. Unless otherwise noted, we use 95%-confidence intervals in this paper. Autocorrelation of the time series is accounted for in the uncertainties following Santer et al. (2000).

3 Century Analysis

We first analyze the long-term trend in $[H_2O]_{entry}$ over the 21^{st} century. To do this, we calculate annual average values of $[H_2O]_{entry}$ and perform a MLR against annual averages of the indices for BDC, QBO and ΔT. All annual averages time series have had the 2000-2010 average subtracted out.

Figure 1 shows that the fits to most of the models generate adjusted R^2 values greater than 0.8. The NIWA-UKCA century MLR has the lowest adjusted R^2, with a value of approximately 0.6. Overall, this result confirms the result of Dessler et al. (2013) that the regression model does an excellent job reproducing the models' $[H_2O]_{entry}$. Because we have left long-term trends in the time series, we will refer to this as the "trended analysis".

3.1 Detrended 21^{st} Century

One concern with the trended analysis is that the $[H_2O]_{entry}$ time series, the BDC, and ΔT indices are all dominated by long-term trends. In such a case, an MLR may produce a high adjusted R^2 even if there is no actual relation between the variables. To eliminate the influence of long-term trends on adjusted R^2, we detrend each variable using a Fourier Transform filter (Donnelly, 2006) to remove long-term variability ($>$ 10 years). We then use the MLR on the detrended $[H_2O]_{entry}$ and the detrended indices. Detrending by removing the long-term linear trend yields similar results.

Figure 1 shows the adjusted R^2 for the detrended calculation. For most of the models, the adjusted R^2 for the detrended MLR is only slightly smaller than that for the trended one. This confirms that the long-term trends in the data tend to inflate the adjusted R^2, at least a bit, and also that the models' interannual variability and long-term trends are well represented by

Atmos. Chem. Phys. Discuss., doi:10.5194/acp-2016-964, 2016
Manuscript under review for journal Atmos. Chem. Phys.
Published: 8 November 2016

Atmospheric Chemistry and Physics Discussions

the same linear model (Equation 1). Large differences do exist for some CCMs. For instance, the CCSRNIES trended century MLR captures approximately 90% of the variance in $[H_2O]_{entry}$, while the detrended century MLR only explains about 40% of interannual variance; the CNRM-CM5-3, NIWA-UKCA, and WACCM show something similar.

3.2 Physical Process Effects

The coefficients from the trended and detrended calculations are listed in Tables 2 and 3 respectively. The product of the regression coefficient and its index quantifies that process' impact on $[H_2O]_{entry}$. As an example, MRI $[H_2O]_{entry}$ increases by about 1.2 ppmv during the 21^{st} century (Figure 2). The regression shows that this is the result of a large increase in $[H_2O]_{entry}$ due to ΔT increases (1.5 ppmv) that is offset by a strengthening BDC, which reduces $[H_2O]_{entry}$ by approximately 0.3 ppmv; this is consistent with the results of Dessler et al. (2013). The regression finds virtually no change in $[H_2O]_{entry}$ in response to the QBO, which does not comport with analyses of observations, which suggests that the QBO causes short-term variations in $[H_2O]_{entry}$ of 0.3 ppmv (Dessler et al., 2014)

Figure 3 shows that $[H_2O]_{entry}$ increases as ΔT increases in all models and that the ΔT regression coefficients are similar for both trended and detrended MLRs. On average, $[H_2O]_{entry}$ increases by about 0.3 ± 0.1 ppmv K^{-1}, with individual models yielding values ranging from about 0.1 to 0.6 ppmv K^{-1}. This confirms that the stratospheric water vapor feedback identified by Dessler et al. (2013) occurs in all CCMs, although the exact magnitude varies.

This figure also shows that the BDC coefficient is generally negative, meaning that a strengthening BDC reduces $[H_2O]_{entry}$. This is consistent with previous research, which showed that a stronger BDC reduces TTL temperatures and lower stratospheric water vapor (Randel et al., 2006; Gilford et al., 2016). The trended and detrended BDC coefficients are similar in sign and magnitude. Two models (CNRM-CM5-3 and NIWA-UKCA) yield positive BDC coefficients, indicating potential problems with these models.

Figure 3 shows that all QBO regression coefficients are small, generally within $\pm$ 0.04 ppmv, with even the sign of the effect in doubt. Interestingly, one of the CCMs not simulating a QBO, CMAM-CCMI, produces the largest QBO regression coefficients of 0.082 ±0.04 and 0.077 ±0.04 ppmv for the trended and detrended calculations, respectively. Among CCMs that do simulate a QBO, the ensemble average QBO regression coefficient does not differ much from the same quantity (approximately 0 ppmv) for the other models. We will discuss this further in the next section.

4 Decadal Analysis

Ideally, we would compare the results of the last section to observations. Unfortunately, we don't have 100 years of observations to test the models against. Instead, we will compare regressions of 10-year segments from the CCMs to regressions of 10-years of observations.

Specifically, we split 21^{st} century of each CCM run into 10 decades (2000-2010, 2010-2020, 2020-2030, 2040-2050, etc.) and fit each individual decade using the regression model (Equation 1). The regression calculation used on each 10-year segment is identical to the century analysis, except monthly averaged anomalies are used instead of annual mean anomalies.

Atmos. Chem. Phys. Discuss., doi:10.5194/acp-2016-964, 2016
Manuscript under review for journal Atmos. Chem. Phys.
Published: 8 November 2016

Atmospheric Chemistry and Physics Discussions

Following Dessler et al. (2014), decadal regression terms are lagged in order to maximize MLR fit: we lag ΔT by 3 months, the BDC by 1 month, and the QBO by 3 months. These lags reflect the time between changes in each index and the impact on $[H_2O]_{entry}$.

Figure 4 shows the median $\pm$ one standard deviation of the ten decadal adjusted R^2 values generated by each CCM. The ensemble average is approximately 0.6 ± 0.25, with some spread among the models. Also plotted are the adjusted R^2 from two regressions of the tropical average Aura Microwave Limb Sounder (MLS) 82-hPa water vapor mixing ratio observations from Dessler et al. (2014). One regression uses Modern-Era Retrospective Analysis for Research and Applications reanalysis (MERRA) data (Rienecker et al., 2011) and the other uses European Centre for Medium-Range Weather Forecasts interim reanalysis (ERAI) (Dee et al., 2011) for the ΔT and BDC indices; the QBO index is standardized anomaly of monthly and zonally averaged equatorial 50-hPa winds obtained from the NOAA Climate Prediction Center (http://www.cpc.ncep.noaa.gov/data/indices). The MLS data covers the time period 2004-2014.

Many of the models have a range of adjusted R^2 values that overlaps with the observational regression However, not all do: the CCSRNIES, CNRM-CM5-3, and NIWA-UKCA have median decadal adjusted R^2 values below 0.4, well below the observational values. It's worth nothing that these models also had issues in the century regressions. The WACCM and LMDZrepro models also have median adjusted R^2 values below the observations.

Figure 5 shows the median and one standard deviation of each coefficient (values are listed in table 4), along with the coefficients from the regression of the MLS data (taken from Dessler et al. (2014)). We find that the CCMs agree unanimously that increases in ΔT are associated with increased $[H_2O]_{entry}$. Overall, though, the CCM ensemble tends to underestimate the observational estimate, although most fall within the observation's 95% confidence intervals. The only models that don't fall within both observational ranges are CCSRNIES, CMAM-CCMI, and CNRM-CM5-3.

In addition, the spread between the different decades for a single model tends to be small, with most CCM decadal ΔT regression coefficient distributions confined to a narrow range of ± 0.1 ppmv K^{-1} around the model's median. This gives us some confidence that the comparison between the CCMs and one decade of observations is meaningful.

Figure 5 shows that there exists a high degree of variability in the CCMs' decadal BDC regression coefficients, with a CCM ensemble average value of about -4$\pm$2 ppmv $(K/Day)^{-1}$, but with individual CCM values ranging between approximately -12 and +5 ppmv $(K/Day)^{-1}$. On all timescales, we expect a strengthening BDC should cool the TTL and reduce $[H_2O]_{entry}$, so the coefficient should be negative. We see that the median is indeed negative for all CCMs except for the CNRM-CM5-3 and NIWA-UKCA, both of which yield a positive median BDC coefficient (these models also generated positive BDC coefficients for the century analysis).

Comparing to observations, we find that the model ensemble does well. This nonetheless hides a significant spread among the models. The CCSRNIES, CCSRNIES-MIROC-3.2, CMAM, CMAM-CCMI, LMDZrepro, MRI-ESM1r1, and WACCM decadal BDC regression coefficients fall within 95% confidence of MERRA, and only CCSRNIES-MIROC-3.2, LMDZrepro, and WACCM fall within 95% confidence interval of ERAI. As with the ΔT coefficient, the spread between the different decades for a single model tends to be small; this again gives us some confidence in our comparisons to analysis of a single decade of observations.

Atmos. Chem. Phys. Discuss., doi:10.5194/acp-2016-964, 2016
Manuscript under review for journal Atmos. Chem. Phys.
Published: 8 November 2016

Atmospheric Chemistry and Physics Discussions

As expected, figure 5 shows that, for CCMs not simulating a QBO, the ensemble average decadal QBO coefficient is approximately 0 ppmv. But even those that do simulate a QBO, as seen in the century analysis, see little impact on $[H_2O]_{entry}$ from it, with an ensemble average of approximately 0.03 ± 0.04 ppmv. This is significantly smaller than the response to the QBO in the observations, and this appears to be a clear deficiency in the model ensemble.

Only CCSRNIES-MIROC3.2 and CMAM-CCMI decadal regressions produce QBO coefficients approaching those from both observational regressions. Again, CMAM-CCMI does not simulate a QBO, and it is not clear to us why the model does so well in this aspect of our analysis.

Previous studies found that the QBO significantly influences TTL temperatures and subsequently $[H_2O]_{entry}$ (Zhou et al., 2001; Geller et al., 2002; Liang et al., 2011), so the lack of response in the model ensemble seems to be a problem for the models. Previous studies have investigated this issue finding that a higher vertical resolution within the stratosphere can help resolve the QBO's impact on the lower stratosphere (Rind et al., 2014; Anstey et al., 2016; Geller et al., 2016). Clearly, this needs to be investigated further.

5 Century and Decadal Regression Coefficient Comparison

One interesting question is whether the regression coefficients from the decadal analyses are related to regression coefficients from century regressions. To answer this, Figure 6 shows the coefficients from the trended century regressions of each CCM plotted against the median of the decadal regressions from the same CCM. Also shown is a linear least-squares fit to the points. As in the last section, uncertainties in the observational coefficients are bound by 95% confidence intervals calculated by Dessler et al. (2014). Uncertainty in the slope, intercept, and century regression predictions are constrained by 95% confidence intervals determined using each least-squares fit.

For the ΔT coefficient, the best fit line is:

$$\beta(\Delta T, century) = 1.21 \pm 0.44 \beta(\Delta T, decade) + 0.13 \pm 0.08 \quad (2)$$

Thus, the ΔT coefficients from the trended MLRs are slightly larger than those from the decadal MLRs. Using values of $\beta(\Delta T, decade)$ from decadal observations and this fit, we can predict $\beta(\Delta T, century)$. From equation 2, the observed $\beta(\Delta T, decade)$ correspond to $\beta(\Delta T, century)$ of 0.50 ± 0.06 and 0.55 ± 0.08 ppmv K^{-1} for MERRA and ERAI indices, respectively.

For the BDC coefficient, the best fit line is:

$$\beta(BDC, century) = 1.16 \pm 0.32 \beta(BDC, decade) + 0.56 \pm 1.56 \quad (3)$$

The BDC coefficients from the trended MLRs are also slightly larger than those from the decadal MLRs. By fitting the observed values of $\beta(BDC, decade)$ through equation 3, we can predict $\beta(BDC, century)$. Using equation 3, the observed values of $\beta(BDC, decade)$ correspond to $\beta(BDC, century)$ of -3.45 ± 1.09 and -2.34 ± 1.09 ppmv $(K/Day)^{-1}$ for MERRA and ERAI indices, respectively.

Atmos. Chem. Phys. Discuss., doi:10.5194/acp-2016-964, 2016
Manuscript under review for journal Atmos. Chem. Phys.
Published: 8 November 2016

Atmospheric Chemistry and Physics Discussions

For the QBO coefficient, the best fit line is:

$$\beta(QBO, century) = 0.75 \pm 0.40 \beta(QBO, decade) + 0.004 \pm 0.01 \quad (4)$$

The QBO coefficients from the trended MLRs are slightly smaller than those from the decadal MLRs. Again, using equation 4, we can predict $\beta(QBO, century)$ using observed values of $\beta(QBO, decade)$. Using equation 4, the observed values of $\beta(QBO, decade)$ correspond to $\beta(QBO, century)$ of 0.09 $\pm$0.03 and 0.09 $\pm$0.02 ppmv for MERRA and ERAI indices, respectively.

6 Conclusions

Climate models predict that tropical lower stratospheric humidity ($[H_2O]_{entry}$) will increase as the climate warms, with important implications for the chemistry and climate of the atmosphere. We described in this paper a new way to evaluate the realism of these model trends. Our method is based on regressing CCM $[H_2O]_{entry}$ time series against three processes (tropospheric temperature (ΔT), the strength of the Brewer-Dobson circulation (BDC), and the phase of the QBO) that have been shown to be important to $[H_2O]_{entry}$. We do this on two separate time-scales: 1) the 21^{st} century, and 2) on decadal timescales.

We find that long-term increase in $[H_2O]_{entry}$ in the CCMs is primarily driven by warming of the troposphere. This is partially offset in most CCMs by an increase in the strength of the Brewer-Dobson circulation, which tends to cool the tropical tropopause layer (TTL). The models show little impact from the QBO, in disagreement with observations; this appears to be a deficiency in the models.

The coefficients from regressions of individual decades in the CCMs can be compared to coefficients from regressions of observations covering a decade. Overall, the CCM ensemble seems to reproduce observations well, except for the fact that the CCMs simulate little response of $[H_2O]_{entry}$ to the QBO, in disagreement with the observations. In addition, the good agreement on average hides some spread among the models, particularly in the response to the BDC.

Our approach provides more insight into model processes than simply comparing $[H_2O]_{entry}$ or TTL temperatures. Our overall conclusions are encouraging — the models appear do a reasonable job simulating variability in $[H_2O]_{entry}$. However, some models have clear problems, e.g., the models that predict $[H_2O]_{entry}$ will increase with a strengthening BDC. In addition, nearly the entire ensemble does not reproduce the observed variations of $[H_2O]_{entry}$ with the phase of the QBO. This analysis should help the modeling groups refine their models' simulations of the 21^{st} century.

7 Data availability

This data can be obtained through the British Atmospheric Data Center (BADC) archive.

Author contributions. KS and AD performed this analysis and wrote most of this manuscript. The other authors contributed information pertaining to their individual models and helped revise this paper.

Atmos. Chem. Phys. Discuss., doi:10.5194/acp-2016-964, 2016
Manuscript under review for journal Atmos. Chem. Phys.
Published: 8 November 2016

Atmospheric Chemistry and Physics Discussions

Competing interests. The authors declare that they have no conflict of interest.

Acknowledgements. This work was supported by NASA grant NNX14AF15G to Texas A&M University. We acknowledge the British Atmospheric Data Center (BADC) for collecting and archiving the CCMVal and CCMI model output. We would like to thank the WACCM group at NCAR and the CNRM-CM5-3 group for model development and making their simulations available to us. Additionally, we would like to thank those involved in GEOSCCM model development, the NASA MAP program, and the high-performance computing resources provided by the NASA Center for Climate Simulation (NCCS). OM acknowledges funding by the New Zealand Royal Society Marsden Fund (grant no. 12-NIW-006). OM and GZ wish to acknowledge the contribution of NeSI high-performance computing facilities to the results of this research. NZ's national facilities are provided by the NZ eScience Infrastructure and funded jointly by NeSI's collaborator institutions and through the Ministry of Business, Innovation & Employment's Research Infrastructure programme (https://www.nesi.org.nz). HA acknowledges the Environment Research and Technology Development Fund, Ministry of Environment, Japan (2–1303) and NEC–SX9/A(ECO) computers at CGER, NIES. The LMDZ-REPRO contribution was supported by the European Project StratoClim (7th framework programme, Grant agreement 603557) and the Grant'SOLSPEC' from the Centre d'Etude Spatiale (CNES).

Atmos. Chem. Phys. Discuss., doi:10.5194/acp-2016-964, 2016
Manuscript under review for journal Atmos. Chem. Phys.
Published: 8 November 2016

Atmospheric Chemistry and Physics Discussions

References

Anstey, J. A., Scinocca, J. F., and Keller, M.: Simulating the QBO in an Atmospheric General Circulation Model: Sensitivity to Resolved and Parameterized Forcing, J. Atmos. Sci., 73, 1649–1665, doi:10.1175/JAS-D-15-0099.1, 2016.

Brewer, A. W.: Evidence for a World Circulation Provided by the Measurements of Helium and Water Vapour Distribution in the Stratosphere., Q. J. R. Meteorol. Soc., 75, 351–363, doi:10.1002/qj.49707532603, 1949.

Castanheira, J. M., Peevey, T. R., Marques, C. A. F., and Olsen, M. A.: Relationships between Brewer-Dobson circulation, double tropopauses, ozone and stratosphere water vapor, Atmos. Chem. Phys., 12, 10 195–10 208, doi:10.5194/acp-12-10195-2012, 2012.

Choiu, E. W., Thomason, L. W., and Chu, W. P.: Variability of Stratospheric Water Vapor Inferred from SAGE II, HALOE, and Boulder (Colorado) Balloon Measurements., J. Climate, 19, 4121–4133, doi:10.1175/JCLI3841.1, 2006.

Dee, D. P., Uppala, S. M., Simmons, A. J., Berrisford, P., Poli, P., Kobayashi, S., Andrae, U., Balmaseda, M. A., Balsamo, G., Bauer, P., Bechtold, P., Beljaars, A. C. M., van de Berg, L., Bidlot, J., Bormann, N., Delsol, C., Dragani, R., Fuentes, M., Geer, A. J., Haimberger, L., Healy, S. B., Hersbach, H., Hólm, E. V., Isaksen, L., Kållberg, P., Köhler, M., Matricardi, M., McNally, A. P., Monge-Sanz, B. M., Morcrette, J.-J., Park, B.-K., Peubey, C., de Rosnay, P., Tavolato, C., Thépaut, J.-N., and Vitart, F.: The ERA-Interim reanalysis: configuration and performance of the data assimilation system, Quarterly Journal of the Royal Meteorological Society, 137, 553–597, doi:10.1002/qj.828, http://dx.doi.org/10.1002/qj.828, 2011.

Dessler, A. E., Schoeberl, M. R., Wang, T., Davis, S. M., and Rosenlof, K. H.: Stratospheric water vapor feedback, PNAS, 110, 18 087–18 091, doi:10.1073/pnas.1310344110, 2013.

Dessler, A. E., Schoeberl, M. R., Wang, T., Davis, S. M., Rosenlof, K. H., and Vernier, J. P.: Variations of stratospheric water vapor over the past three decades, J. Geophys. Res. Atmos., 119, 12 588–12 598, doi:10.1002/2014JD021712, 2014.

Donnelly, D.: The Fast Fourier Transform For Experimentalist, Part V: Filters., Computing in Science and Engineering, 8, 92–95, doi:10.1109/MCSE.2006.14, 2006.

Dunkerton, T.: On the Mean meridional mass motions of the stratosphere and mesosphere., J. Atmos. Sci., 58, 7–25, doi:10.1175/1520-0469(1978)035<2325:OTMMMM>2.0.CO;2, 2001.

Fueglistaler, S. and Haynes, P. H.: Control of interannual and longer-term variability of stratospheric water vapor, J. Geophys. Res., 110, doi:10.1029/2005JD006019, 2005.

Fueglistaler, S., B.Legras, Beljaars, A., Morcrette, J. J., Simmons, A., Tompkins, A. M., and Uppala, S.: The diabatic heat budget of the upper troposphere and lower/mid stratosphere in ECMWF reanalyses., Q. J. R. Meteorol. Soc., 135, 21–37, doi:10.1002/qj.361, 2009a.

Fueglistaler, S., Dessler, A. E., Dunkerton, T. J., Folkins, I., Fu, Q., and Mote, P. W.: Tropical tropopause layer, Rev. Geophys., 47, doi:10.1029/2008RG000267, 2009b.

Fueglistaler, S., Liu, Y. S., Flannaghan, T. J., Ploeger, F., and Haynes, P. H.: Departure from Clausius-Clapeyron scaling of water entering the stratosphere in response to changes in tropical upwelling, J. Geophys. Res. Atmos., 119, 1962–1972, doi:10.1002/2013JD020772, 2014.

Geller, M. A., Zhou, X., and Zhang, M.: Simulations of the Interannual Variability of Stratospheric Water Vapor, J. Atmos. Sci., 59, 1076–1085, doi:10.1175/1520-0469(2002)059<1076:SOTIVO>2.0.CO;2, 2002.

Geller, M. A., Zhou, T., Shindell, D., Ruedy, R., Aleinov, I., Nazarenko, L., Tausnev, N. L., Kelley, M., Sun, S., Cheng, Y., Field, R. D., and Faluvegi, G.: Modeling the QBO—Improvements resulting from higher- model vertical resolution, J. Adv. Model. Earth Syst., 8, doi:10.1002/2016MS000699, 2016.

Atmos. Chem. Phys. Discuss., doi:10.5194/acp-2016-964, 2016
Manuscript under review for journal Atmos. Chem. Phys.
Published: 8 November 2016

Atmospheric Chemistry and Physics Discussions

Gilford, D. M., Solomon, S., and Portmann, R. W.: Radiative Impacts of the 2011 Abrupt Drops in Water Vapor and Ozone in the Tropical Tropopause Layer, J. Climate, 29, 595–612, doi:10.1175/JCLI-D-15-0167.1, 2016.

IPCC: Climate Change 2001: The Scientific Basis: Contribution of Working Group 1 to the Third Assessment Report of the Intergovernmental Panel on Climate Change, Tech. rep., Intergovernmental Panel on Climate Change (IPCC), New York, 2001.

Kawatani, Y., Lee, J. N., and Hamilton, K.: Interannual Variations of Stratospheric Water Vapor in MLS Observations and Climate Model Simulations., J. Atmos. Sci., 71, 4072–4085, doi:10.1175/JAS-D-14-0164.1, 2014.

Khosrawi, F., Müller, R., Urban, J., Proffitt, M. H., Stiller, G., Kiefer, M., Lossow, S., Kinnison, D., Olschewski, F., Riese, M., and Murtagh, D.: Assessment of the interannual variability and influence of the QBO and upwelling on tracer–tracer distributions of N_2O and O_3 in the tropical lower stratosphere, Atmos. Chem. Phys., 13, 3619–3641, doi:10.5194/acp-13-3619-2013, http://www.atmos-chem-phys.net/13/3619/2013/, 2013.

Liang, C. K., Eldering, A., Gettelman, A., Tian, B., Wong, S., Fetzer, E. J., and Liou, K. N.: Record of tropical interannual variability of temperature and water vapor from a combined AIRS-MLS data set, J. Geophys. Res. Atmos., 116, n/a–n/a, doi:10.1029/2010JD014841, http://dx.doi.org/10.1029/2010JD014841, d06103, 2011.

Meinshausen, M., Smith, S. J., Calvin, K., Daniel, J. S., Kainuma, M. L. T., Lamarque, J.-F., Matsumoto, K., Montzka, S. A., Raper, S. C. B., Riahi, K., Thomson, A., Velders, G. J. M., and van Vuuren, D. P. P.: The RCP greenhouse gas concentrations and their extensions from 1765 to 2300, Climatic Change, 109, 213–241, doi:10.1007/s10584-011-0156-z, 2011.

Morgenstern, O., Giorgetta, M. A., Shibata, K., Eyhring, V., Waugh, D. W., Shepherd, T. G., Akiyoshi, H., Austin, J., Baumgaertner, A. J. G., Bekki, S., Braesicke, P., Brühl, C., Chipperfield, M. P., Cugnet, D., Dameris, M., Dhomse, S., Frith, S. M., Garny, H., Gettleman, A., Hardiman, S. C., Hegglin, M. I., Jöckel, P., Kinnison, D. E., Lamarque, J. F., Mancini, E., Manzini, E., Marchand, M., Michou, M., Nakamura, T., Nielsen, J. E., Olivié, D., Pitari, G., Plummer, D. A., Rozanov, E., Scinocca, J. F., Smale, D., Teyssèdre, H., Toohey, M., Tian, W., and Yamashita, Y.: Review of the formulation of present-generation stratospheric chemistry-climate models and associated external forcings, J. Geophys. Res., 115, doi:10.1029/2009JD013728, 2010.

Morgenstern, O., Hegglin, M. I., Rozanov, E., O'Connor, F. M., Abrams, N. L., Akkyoshi, H., Archibald, A. T., Bekki, S., Butchart, N., Chipperfield, M. P., Deushi, M., Dhomse, S. S., Garcia, R. R., Hardiman, S. C., Horowitz, L. W., Jockel, P., Josse, B., Kinnison, D., Lin, M. Y., Mancini, E., Manyin, M. E., Marchand, M., Marecal, V., Michou, M., Pitari, L. D. O. N. G., Plummer, D. A., Revell, L. E., Saint-Martin, D., Schofield, R., Stenke, A., Stone, K., Sudo, K., Tanaka, T. Y., Tilmes, S., Yamashita, Y., Yoshida, K., and Zeng, G.: Review of the global models used within the Chemistry-Climate Model Initiative (CCMI), GMD, doi:10.5194/gmd-2016-199, 2016.

Mote, P. W., Rosenlof, K. H., McIntyre, M. E., Carr, E. S., Gille, J. C., Holton, J. R., Kinnersley, J. S., Pumphrey, H. C., III, J. M. R., and Waters, J. W.: An atmospheric tape recorder: The imprint of tropical tropopause temperatures on stratospheric water vapor, J. Geophys. Res. Atmos., 101, 3989–4006, doi:10.1029/95JD03422, 1996.

O'Sullivan, D. and Dunkerton, T. J.: The influence of the quasi-biennial oscillation on global constituent distributions, J. Geophys. Res. Atmos., 102, 21 731–21 743, doi:10.1029/97JD01689, http://dx.doi.org/10.1029/97JD01689, 1997.

Randel, W. J., Wu, F., Russell, J. M., Roche, A., and Waters, J. W.: Seasonal cycles and QBO variations in stratospheric CH4 and H2O observed in UARS HALOE data, J. Atmos. Sci., 55, doi:10.1175/1520-0469(1998)055<0163:SCAQVI>2.0.CO;2, 1998.

Randel, W. J., Wu, F., Vömel, H., Nedoluha, G. E., and Forster, P.: Decreases in stratospheric water vapor after 2001: Links to changes in the tropical tropopause and the Brewer-Dobson circulation, J. Geophys. Res. Atmos., 111, doi:10.1029/2005JD006744, 2006.

Atmos. Chem. Phys. Discuss., doi:10.5194/acp-2016-964, 2016
Manuscript under review for journal Atmos. Chem. Phys.
Published: 8 November 2016

Rienecker, M., Suarez, M. J., Gelaro, R., Todling, R., Bacmeister, J., Liu, E., Bosilovich, M. G., Schubert, S. D., Takacs, L., Kim, G. K., Bloom, S., Chen, J., Collins, D., Conaty, A., and Silva, A. D.: MERRA: Nasa 's Modern-Era Retrospective Analysis for Research and Applications, J. Climate, 24, 3624–3648, doi:10.1175/JCLI-D-11-00015.1, 2011.

Rind, D., Jonas, J., Balachandran, N. K., Schmidt, G. A., and Lean, J.: The QBO in two GISS global climate models: 1. Generation of the QBO, Journal of Geophysical Research: Atmospheres, 119, 8798–8824, doi:10.1002/2014JD021678, http://dx.doi.org/10.1002/2014JD021678, 2014JD021678, 2014.

Santer, B. D., Wigley, T. M. L., Boyle, J. S., Gaffin, D. J., Hnilo, J. J., Nychka, D., Parker, D. E., and Taylor, K. E.: Statistical significance of trends and trend differences in layer-average atmospheric temperature time series, J. Geophys. Res., 105, 7337–7356, doi:10.1029/1999jd901105, 2000.

SPARC: SPARC CCMVal Report on the Evaluation of Chemistry-Climate Models, Tech. rep., Stratosphere-troposphere Processes and their role in climate (SPARC), http://www.sparc-climate.org/publications/sparc-reports/, 2010.

Tao, M., Konopka, P., Ploeger, F., Grooß, J.-U., Müller, R., Volk, C. M., Walker, K. A., and Riese, M.: Impact of the 2009 major sudden stratospheric warming on the composition of the stratosphere, Atmos. Chem. Phys., 15, 8695–8715, doi:10.5194/acp-15-8695-2015, http://www.atmos-chem-phys.net/15/8695/2015/, 2015.

WMO: Scientific Assessment of Ozone Depletion: 2006, Tech. Rep. 50, Global Ozone Research and Monitoring Project, Geneva, Switzerland, 2007.

WMO: Scientific Assessment of Ozone Depletion: 2014, Tech. Rep. 56, Global Ozone Research and Monitoring Project, Geneva, Switzerland, 2014.

Zhou, X. L., Geller, M. A., and Zhang, M. H.: Tropical Cold Point Tropopause Characteristics Derived from ECMWF Reanalyses and Soundings, J. Climate, 14, 1823?–1838, doi:10.1175/1520-0442(2001)014<1823:TCPTCD>2.0.CO;2, 2001.

Atmos. Chem. Phys. Discuss., doi:10.5194/acp-2016-964, 2016
Manuscript under review for journal Atmos. Chem. Phys.
Published: 8 November 2016

Atmospheric Chemistry and Physics Discussions

Table 1. CCMs used in this analysis. The resolution is listed as (lat x lon x number of pressure levels). 31 vertical levels indicates CCM data is given on isobaric levels, while CCMs simulating data on >31 levels are given on sigma (hybrid-pressure) levels

Chemistry Climate Model Properties				
CCM	Resolution	Dataset	Contains QBO	Institution
CCSRNIES	2.8° x 2.8° x 31	CCMVal-2	No	NIES, Tsukuba, Japan
CCSRNIES-MIROC3.2	2.8° x 2.8° x 34	CCMI-1	Yes	NIES, Tsukuba, Japan
CMAM	5.5° x 5.6° x 31	CCMVal-2	No	EC, Canada
CMAM-CCMI	3.7° x 3.8° x 71	CCMI-1	No	EC, Canada
CNRM-CM5-3	2.8° x 2.8° x 31	CCMI-1	No	Meteo-France; France
GEOSCCM	2.0° x 2.5° x 31	CCMVal-2	No	NASA/GSFC, USA
GEOSCCM-CCMI	2.0° x 2.5° x 72	CCMI-1	Yes	NASA/GSFC, USA
LMDZrepro	2.5° x 3.8° x 31	CCMVal-2	No	IPSL, France
MRI	2.8° x 2.8° x 31	CCMVal-2	Yes	MRI, Japan
MRI-ESM1r1	2.8° x 2.8° x 80	CCMI-1	Yes	MRI, Japan
NIWA-UKCA	2.5° x 3.8° x 31	CCMI-1	Yes	NIWA, NZ
WACCM	1.9° x 2.5° x 31	CCMVal-2	No	NCAR, USA

Atmos. Chem. Phys. Discuss., doi:10.5194/acp-2016-964, 2016
Manuscript under review for journal Atmos. Chem. Phys.
Published: 8 November 2016

Atmospheric Chemistry and Physics Discussions

Table 2. Coefficients from regressions of trended $[H_2O]_{entry}$ time series

Trended Regression Coefficients			
CCM	ΔT	BDC	QBO
CCSRNIES	0.06±0.01	-0.67±0.95	1.7x10^{-2}±0.01
CCSRNIES-MIROC3.2	0.40±0.06	-3.4±1.9	3.5x10^{-2}±0.04
CMAM	0.26±0.02	-5.7±1.1	8.0x10^{-4}±0.03
CMAM-CCMI	0.22±0.05	-3.8±2.6	8.2x10^{-2}±0.04
CNRM-CM5-3	0.27±0.13	3.7±5.4	1.9x10^{-2}±0.07
GEOSCCM	0.38±0.03	-6.7±0.82	-1.3x10^{-2}±0.01
GEOSCCM-CCMI	0.27±0.03	-6.6±0.96	5.2x10^{-3}±0.02
LMDZrepro	0.55±0.04	-8.3±2.1	1.4x10^{-2}±0.04
MRI	0.57±0.03	-12.±1.3	-4.1x10^{-3}±0.03
MRI-ESM1r1	0.36±0.05	-3.1±1.4	1.7x10^{-2}±0.03
NIWA-UKCA	0.20±0.07	4.3±4.6	-1.0x10^{-2}±0.07
WACCM	0.24±0.04	-3.5±1.2	1.5x10^{-2}±0.03

The units of ΔT, BDC, and QBO are ppmv K^{-1}, ppmv $(K/Day)^{-1}$, and ppmv. The uncertainty is the 95% confidence interval.

Atmos. Chem. Phys. Discuss., doi:10.5194/acp-2016-964, 2016
Manuscript under review for journal Atmos. Chem. Phys.
Published: 8 November 2016

Atmospheric Chemistry and Physics Discussions

Table 3. Coefficients from regressions of detrended $[H_2O]_{entry}$ time series

Detrended Regression Coefficients			
CCM	ΔT	BDC	QBO
CCSRNIES	0.05±0.02	-0.67±0.67	1.7x10^{-2}±0.01
CCSRNIES-MIROC3.2	0.30±0.05	-4.3±0.83	2.8x10^{-2}±0.01
CMAM	0.26±0.03	-5.3±0.84	7.0x10^{-4}±0.02
CMAM-CCMI	0.26±0.05	-3.7±1.1	7.7x10^{-2}±0.04
CNRM-CM5-3	0.19±0.05	0.20±1.1	-3.3x10^{-2}±0.01
GEOSCCM	0.31±0.04	-6.6±0.65	-1.0x10^{-2}±0.01
GEOSCCM-CCMI	0.25±0.04	-7.1±0.71	4.4x10^{-3}±0.01
LMDZrepro	0.59±0.05	-5.4±1.1	-5.5x10^{-3}±0.03
MRI	0.52±0.03	-11.±1.0	-4.6x10^{-4}±0.02
MRI-ESM1r1	0.33±0.05	-4.3±0.61	5.5x10^{-3}±0.01
NIWA-UKCA	0.15±0.08	2.9±1.6	-1.0x10^{-2}±0.02
WACCM	0.23±0.05	-3.5±0.80	1.5x10^{-2}±0.02

The units of ΔT, BDC, and QBO are ppmv K^{-1}, ppmv $(K/Day)^{-1}$, and ppmv. The uncertainty is the 95% confidence interval.

Atmos. Chem. Phys. Discuss., doi:10.5194/acp-2016-964, 2016
Manuscript under review for journal Atmos. Chem. Phys.
Published: 8 November 2016

Atmospheric Chemistry and Physics Discussions

Table 4. Median coefficients from the decadal regressions of $[H_2O]_{entry}$ monthly anomalies

Decadal Regression Coefficients			
CCM	ΔT	BDC	QBO
CCSRNIES	0.03±0.04	-1.23±1.34	5.26x10^{-3}±0.02
CCSRNIES-MIROC3.2	0.10±0.17	-3.29±1.44	6.05x10^{-2}±0.01
CMAM	0.19±0.09	-6.06±1.34	2.75x10^{-3}±0.03
CMAM-CCMI	0.01±0.10	-4.70±1.29	6.13x10^{-2}±0.01
CNRM-CM5-3	0.06±0.14	2.89±1.44	1.84x10^{-2}±0.02
GEOSCCM	0.17±0.10	-6.31±1.19	-1.47x10^{-2}±0.03
GEOSCCM-CCMI	0.11±0.16	-8.00±1.89	2.42x10^{-2}±0.02
LMDZrepro	0.31±0.19	-2.71±2.71	1.27x10^{-2}±0.01
MRI	0.35±0.09	-8.78±2.91	-6.56x10^{-3}±0.06
MRI-ESM1r1	0.19±0.12	-4.72±0.71	1.17x10^{-2}±0.03
NIWA-UKCA	0.05±0.29	2.11±3.26	-1.88x10^{-2}±0.04
WACCM	0.15±0.12	-2.25±0.85	3.84x10^{-2}±0.03
MLS/ERAI	0.34±0.17	-2.5±0.83	1.1x10^{-1}±0.04
MLS/MERRA	0.30±0.20	-3.5±1.6	1.2x10^{-1}±0.05

The units of ΔT, BDC, and QBO are ppmv K^{-1}, ppmv $(K/Day)^{-1}$, and ppmv. The uncertainty represents the variability (one standard deviation) in the set of coefficients produced by each CCM. For observations, the error bars represent 95% confidence.

Atmos. Chem. Phys. Discuss., doi:10.5194/acp-2016-964, 2016
Manuscript under review for journal Atmos. Chem. Phys.
Published: 8 November 2016

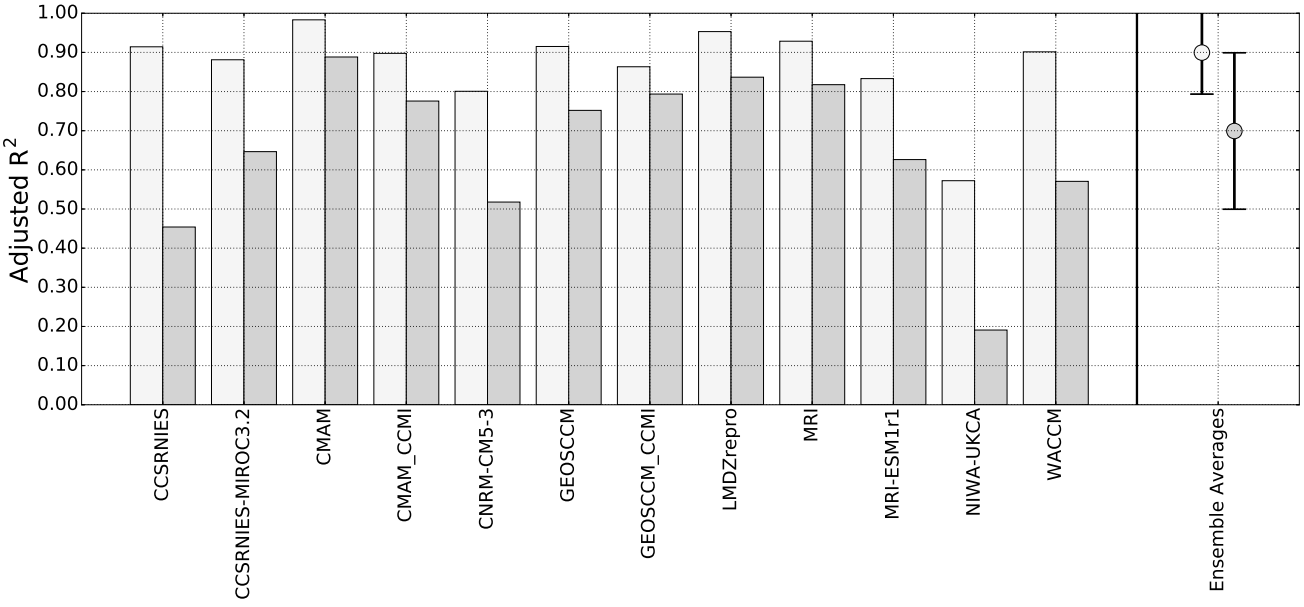

Figure 1. Bars corresponds to trended (light grey) and detrended (dark grey) adjusted R^2 values for annual-averaged data. The light grey circle represents the CCM ensemble mean trended adjusted R^2 value, while the dark grey circle represents to the CCM ensemble mean detrended adjusted R^2 value. Error bars on ensemble means corresponds to the $\pm$ one standard deviation of the CCM ensemble.

Atmos. Chem. Phys. Discuss., doi:10.5194/acp-2016-964, 2016
Manuscript under review for journal Atmos. Chem. Phys.
Published: 8 November 2016

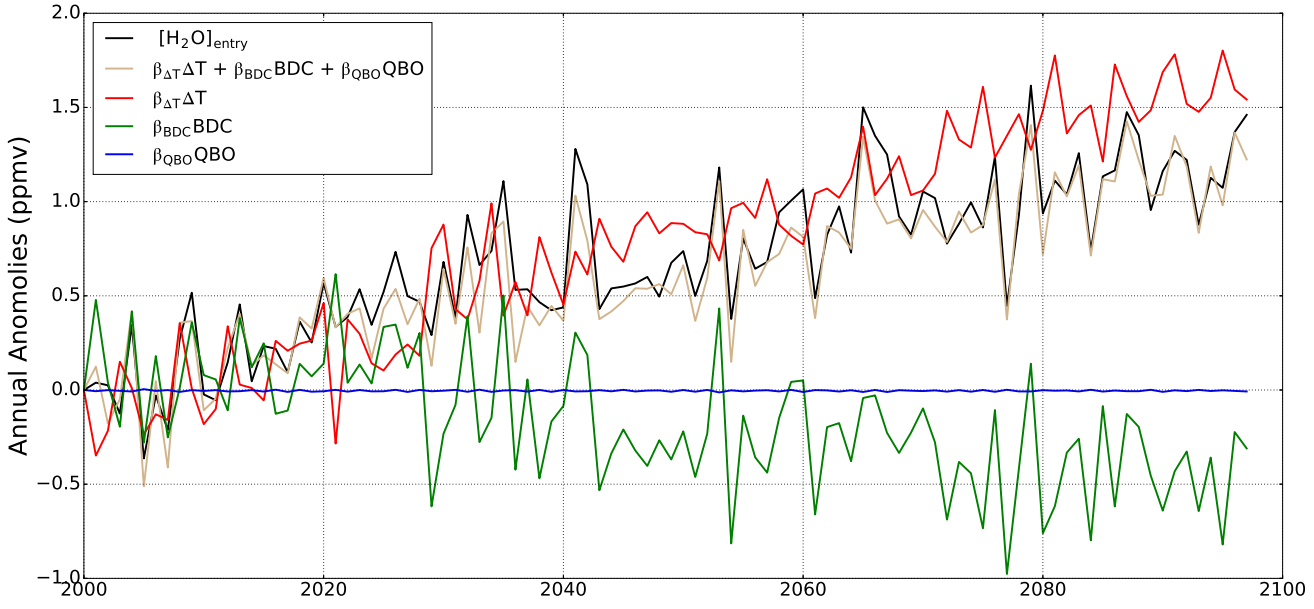

Figure 2. Time series of annual-averaged anomalies of $[H_2O]_{entry}$ from the MRI (black), and its reconstruction using a multivariate linear regression (brown). The red, green, and blue lines are the ΔT, BDC, and QBO terms from the regression, respectively.

Atmos. Chem. Phys. Discuss., doi:10.5194/acp-2016-964, 2016
Manuscript under review for journal Atmos. Chem. Phys.
Published: 8 November 2016

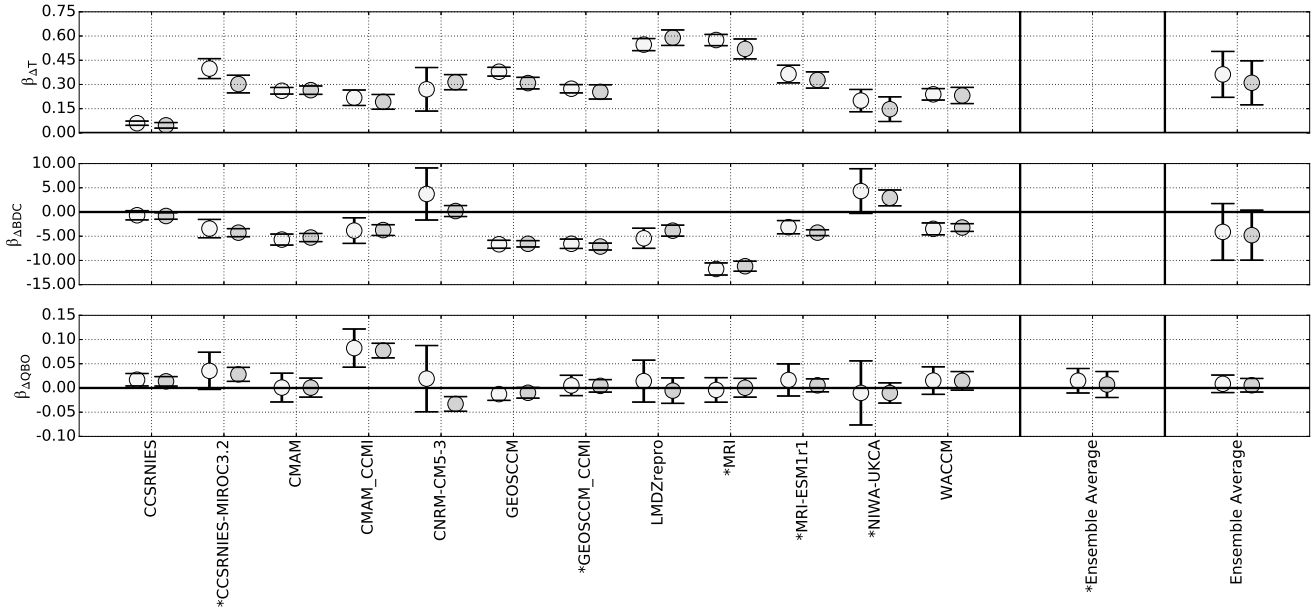

Figure 3. Circles represents the detrended (light grey) and trended (dark grey) coefficients for each model, and error bars correspond to 95^{th} percentile confidence interval bounding each regression coefficient. An asterisk indicates models simulating a QBO. An asterisk on the ensemble mean corresponds to the average QBO coefficient for only models simulating a QBO, while the ensemble mean with no asterisk corresponds to the average of all model coefficients. The ensemble mean coefficients are also represented by a circle, with associated error bars correspond to ±one standard deviation of the ensemble set of coefficients. The units of $\beta_{\Delta t}$,β_{BDC}, and β_{QBO} are ppmv/K, ppmv/(K/Day), and ppmv, respectively.

Atmos. Chem. Phys. Discuss., doi:10.5194/acp-2016-964, 2016
Manuscript under review for journal Atmos. Chem. Phys.
Published: 8 November 2016

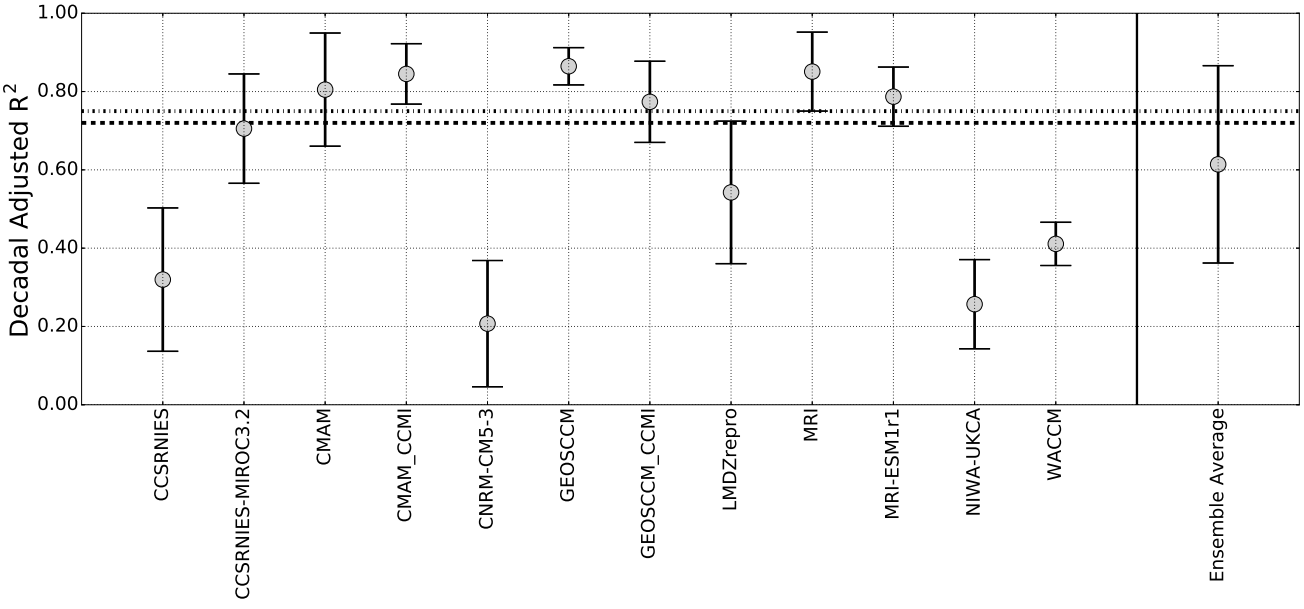

Figure 4. Circles represent the median of the adjusted R^2 value of the decadal fits. Errors correspond to the $\pm$ one standard deviation of the adjusted R^2 values. The CCM ensemble average is also plotted, along with error bars corresponding to $\pm$ one standard deviation of ensemble set of decadal adjusted R^2 values. The lines are adjusted R^2 values from observations combined with reanalysis (ERAI (dotted) and MERRA (dashed)) from Dessler et al. (2014).

Atmos. Chem. Phys. Discuss., doi:10.5194/acp-2016-964, 2016
Manuscript under review for journal Atmos. Chem. Phys.
Published: 8 November 2016

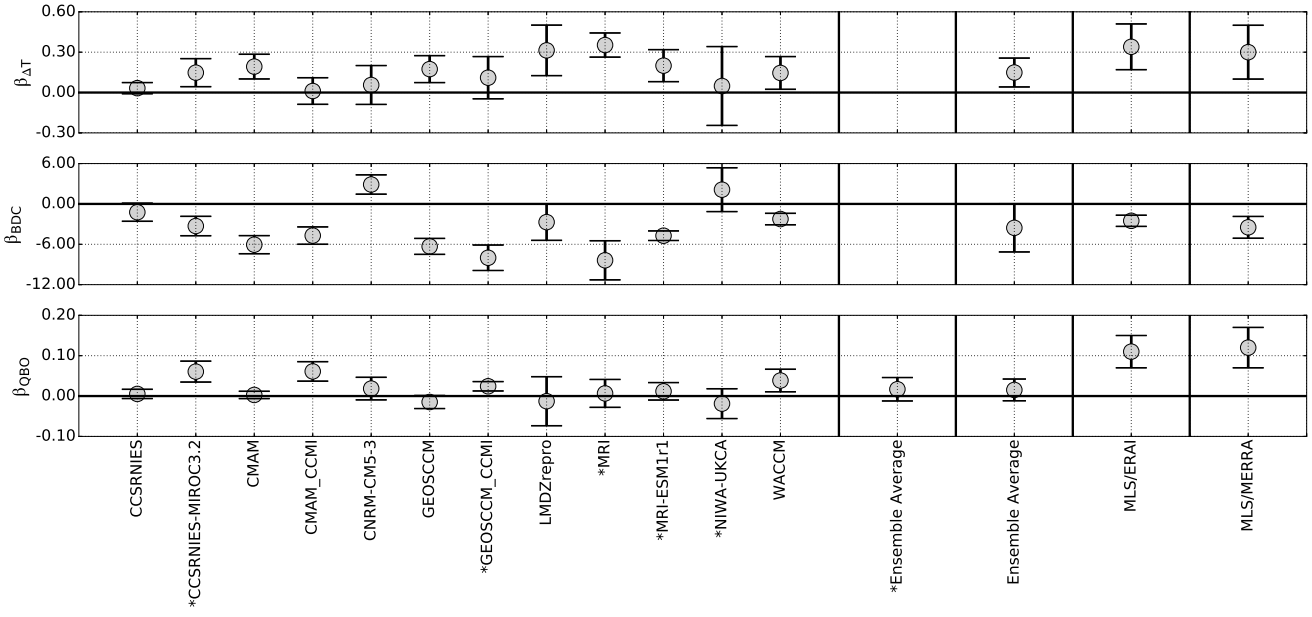

Figure 5. Circles represent the median decadal regression coefficient from each CCM, and error bars correspond to ± one standard deviation. An asterisk indicates that the model simulates a QBO. An asterisk corresponding to the ensemble mean corresponds to the average QBO coefficient for only models simulating a QBO, while the ensemble mean with no asterisk corresponds to an average of all model coefficients. The ensemble mean coefficients are also represented by a circle, with associated error bars correspond to ±one standard deviation of the ensemble set of coefficients. Estimates from observations combined with reanalysis (Dessler et al., 2014) shown, along with 95^{th} percentile confidence interval. The units of $\beta_{\Delta t}$,β_{BDC}, and β_{QBO} are ppmv/K, ppmv/(K/Day), and ppmv, respectively.

Atmos. Chem. Phys. Discuss., doi:10.5194/acp-2016-964, 2016
Manuscript under review for journal Atmos. Chem. Phys.
Published: 8 November 2016

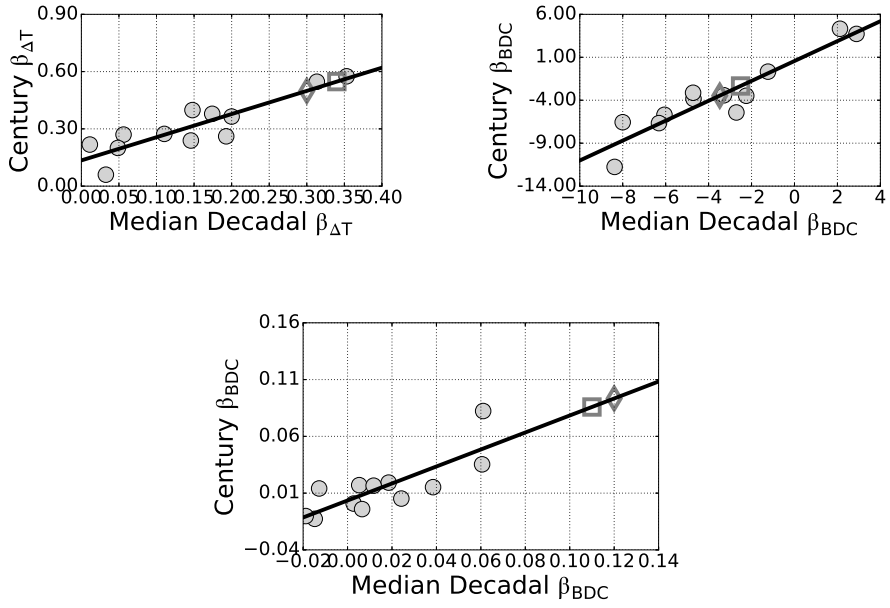

Figure 6. (Top Left) Scatter plots of trended ΔT regression coefficients (ppmv K^{-1}) vs. median decadal ΔT regression coefficients (ppmv K^{-1}) from each CCM. (Top Right) Same as top, but for BDC coefficients. (Bottom Middle) Same as top left and top right, but for QBO coefficient . Black lines in all plots correspond to a best fit line between the trended and decadal coefficients, and the observational coefficients ERAI (square) and MERRA (diamond) are fitted to each line (from Dessler et al. (2014)).